ELSEVIER

Aquacultural Engineering 18 (1998) 201–217

aquacultural engineering

Modeling the thermal characteristics of greenhouse pond systems

S. Zhu [a,*], J. Deltour [b], S. Wang [a]

[a] *Department of Agricultural Engineering, Zhejiang Agricultural University, Hangzhou 310029, P.R. China*

[b] *Faculté Universitaire des Sciences Agronomiques, B-5030 Gembloux, Belgium*

Received 6 November 1997; accepted 20 May 1998

Abstract

Greenhouse pond systems (GPS) can provide a good alternative for maintaining water temperature in aquacultural facilities. However, their thermal characteristics are not well understood. The GPS model advanced in this paper describes the evolution of various heat and water vapor transfer fluxes, temperature and humidity at a given site under various climatic conditions. Simulation results show that, in a 1-m pond, a passive polyethylene GPS can yield a 5.2°C increase in water temperature compared with outside air temperature. The night temperature of the internal air in a passive GPS can be maintained a few degrees higher than that in a horticultural greenhouse. The main heat losses of the water in the GPS are thermal radiation to the cover, convection from the cover to the external air, and thermal radiation from the cover to the sky. Reducing these three heat flux densities is the principal measure for maintaining water temperature or saving energy in a GPS. Water condensation frequently occurs on the inner surface of the cover, which makes highly thermal-radiation-transparent covering materials like polyethylene become opaque to thermal radiation and behave like low emissivity glass. Polyethylene is thus a more sound material for the GPS cover than glass. Mean water temperature in a passive polyethylene GPS is 0.6°C higher than that in a glass GPS, while, in an active polyethylene GPS, the total heat demand is 9.2% lower than that in a glass GPS. From a temperature maintenance point of view, polyvinyl chloride is almost as effective as polyethylene. This model can provide a useful tool for optimum control of water temperature and evaluation of the economic potential for the active GPS.

Keywords: Aquaculture pond; Greenhouse; Heat balance; Model; Simulation

* Corresponding author. Present address: Bio-systems Engineering, Washington State University, Pullman, WA 99164-6120, USA. Tel.: +1 509 3350380; fax: +1 509 3352722; e-mail: zhusm@mail.wsu.edu

0144-8609/98/$19.00
PII S0144-8609(98)00031-4

1. Introduction

Greenhouse pond systems (GPS), used as hatchery, nursery, over-wintering and highly intensive aquaculture facilities, can provide a good alternative for the maintenance of water temperature, yet very few articles in this field have been found in the literature. To date, most pond greenhouses used for aquacultural purposes are copied from those used in horticulture. The thermal characteristics of the GPS are not well understood.

Dynamic simulation is regarded as one of the most powerful approaches to understanding the interactions of a complex system (Cuenco, 1989). Modeling studies on greenhouse climates for horticultural purposes have been carried out for a long time. A number of dynamic models have been developed (Takakura et al., 1971; Kindelan, 1980; Bot, 1983; Deltour et al., 1985; de Halleux, 1989). Of these, the GGDM (Gembloux Greenhouse Dynamic Model) is a powerful model for analyzing the climatic characteristics of horticultural greenhouses (de Halleux, 1989; de Halleux et al., 1985, 1991; Deltour et al., 1985; Nijskens et al., 1991; Pirard et al., 1993; Pieters and Deltour, 1997).

Pond temperature has been modeled by several authors (Klemetson and Rogers, 1985; Cathcart and Wheaton, 1987; Losordo and Piedrahita, 1991; Zhu et al., 1998). The MAPT model by Klemetson and Rogers (1985) was developed for predicting aquacultural pond temperatures throughout the year. Assuming completely airtight conditions (no wind and 100% relative humidity) over the pond surface, the model also allowed the comparison of heat loss reduction for ponds covered by glasshouses, plastic films, etc. Reportedly, a greenhouse or a plastic shelter could achieve a 2.8–4.4°C increase in water temperature for each month of the year when compared with an open-air pond (Klemetson and Rogers, 1985). Little and Wheaton (1987) used a solar-energy-based program to predict water temperature in a greenhouse-covered aquaculture pond. It was expected that, on an average, a 9–10°C increase in water temperature could be achieved by adding a greenhouse cover. The results from the two models seem to be significantly different.

In addition, a few studies have been reported in the literature on the basin solar stills, which are used to produce fresh water from brackish water (Mowla and Karimi, 1995; Shawaqfeh and Farid, 1995; Sartori, 1996). The stills are somewhat similar to the GPS in heat and water vapor transfers, but the water depth in the basin is usually lower than 0.05 m.

The objective of this study was to develop a one-dimensional dynamic model of the GPS for: (1) simulation of the evolution of temperature, relative humidity, heat energy and water vapor transfer fluxes under various climatic conditions, (2) comparison between GPSs with different covering materials.

2. Description of the model

Our GPS model is developed on the basis of the GGDM and the pond water temperature model of Zhu et al. (1998). A detailed introduction to the methods and results in the GGDM can be found in Deltour et al. (1985), de Halleux (1989), de Halleux et al. (1991) and Nijskens et al. (1991). A brief description of the GPS model is given below, while the modifications for the special phenomena due to the pond water instead of the vegetation layer are presented in full detail.

The model is based on the fundamental mechanisms that govern the dynamic exchange or storage of heat and water vapor between the various layers assumed to be homogeneous and infinite in the horizontal plane. In the GPS model, the system is divided into four internal layers (the cover, the internal air, the water and the soil) and three boundary layers (the sky, the external air and the subsoil) (Fig. 1). The interactions between the layers involve heat transfers by convection, latent heat exchange, thermal radiation, solar radiation and conduction. Solar radiation reaches the cover, the water and the pond bottom. Thermal radiation exchanges happen in between the water surface and the cover, and partially the sky, and in between the cover and the sky. Heat conduction takes place exclusively between soil and subsoil layers. Convection and latent heat transfers occur between the air and the water surface, and the inner and outer cover surfaces, as well as from internal to external air, caused by ventilation or air leakage. The convection heat transfer coefficient between the air and the cover or water surface is calculated as:

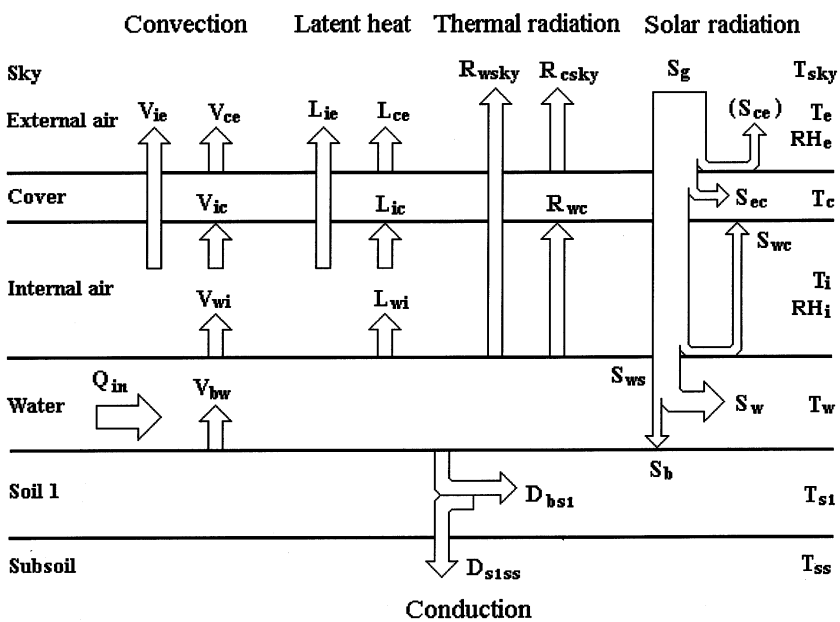

Fig. 1. Diagram of the heat transfer fluxes in the greenhouse pond system model.

Table 1
Nusselt number for laminar and turbulent flow in natural and forced convection mode past a flat plate (Monteith and Unsworth, 1990)

	Laminar	Turbulent
$(Gr/Re^2) \geq 16)$ Natural convection	$(Re \leq 5 \times 10^4)$ $Nu = 0.54(Gr\ Pr)^{1/4}$	$(Re > 5 \times 10^4)$ $Nu = 0.14(Gr\ Pr)^{1/3}$
$(0.1 < Gr/Re^2 < 16)$ Mixed convection		
$(Gr/Re^2 \leq 0.1)$ Forced convection	$(Gr \dot{+} 10^8)$ $Nu = 0.67Re^{1/2}Pr^{1/3}$	$(Gr > 10^8)$ $Nu = 0.036Re^{4/5}Pr^{1/3}$

$$h_v = Nu \frac{\lambda}{d} \tag{1}$$

Where the Nusselt number (Nu) is expressed as in Table 1, according to the fluid dynamic theory described by Monteith and Unsworth (1990). The details of the calculation for the above heat fluxes can be found in Nijskens et al. (1984), de Halleux (1989), Pieters and Deltour (1997) and Zhu et al. (1998).

For the water layer, the heat storage or dissipation flux density results from the difference between the incoming flux densities [solar radiation (S_w), convection from pond bottom (V_{bw}) and heat energy input (Q_{in})], and the outgoing flux densities [convection (V_{wi}) and evaporation (L_{wi}) towards the internal air, radiation to the cover (R_{wc}) and, for a partially transparent cover, to the sky (R_{wsky})]. The heat balance equation of the water layer is thus derived as:

$$\rho_w C_w D_w \frac{dT_w}{dt} = S_w + V_{bw} + Q_{in} - V_{wi} - L_{wi} - R_{wc} - R_{wsky} \tag{2}$$

The solar radiation absorbed by the surface of pond bottom (S_b) supplies heat energy to the water by convection (V_{bw}) and to the soil layer by conduction (D_{bs1}) (Fig. 1). Since there is no heat storage in the pond's bottom surface, the heat balance can be expressed as:

$$V_{bw} + D_{bs1} = S_b \tag{3}$$

Thus:

$$\begin{aligned} S_w + V_{bw} &= S_w + S_b - D_{bs1} \\ &= S_{ws} - D_{bs1} \end{aligned} \tag{4}$$

Where S_{ws} is the solar radiation flux density penetrating the water surface. Therefore, Eq. (2) becomes:

$$\rho_w C_w D_w \frac{dT_w}{dt} = S_{ws} + Q_{in} - D_{bs1} - V_{wi} - L_{wi} - R_{wc} - R_{wsky} \tag{5}$$

There are two types of GPS involved: the passive GPS in which the water temperature varies as affected by the balance of the heat fluxes, as expressed in Eq. (5) where no heat energy is input ($Q_{in} = 0$); and the active GPS where the heating load contributes to the overall thermal equilibrium to keep water temperature above a preset point (T_{wset}). For the active GPS simulation, water temperature is checked at the end of each time step. If the calculated water temperature is higher than or equal to the set point, the heat input is not needed. Otherwise, the water temperature is re-valued to the set point, and the heat input flux density is calculated with:

$$Q_{in} = D_{bs1} + V_{wi} + L_{wi} + R_{wc} + R_{wsky} - S_{ws} \tag{6}$$

The impact of water condensation on the thermal radiation behavior of the cover is carefully considered in the GPS model. For a completely wet surface, the radiation parameters of the material are replaced with those of water, which is totally opaque to thermal radiation. For a partially wet surface, an equivalent surface coverage factor of water (p) is introduced to express the wet fraction of the surface as described in Pieters et al. (1996). In this case, the cover behaves as if a fraction (p) of its surface were wet and a fraction ($1-p$) were dry, and the radiation properties of the surface, the thermal transmissivity (τ_{Rcw}) and emissivity (ϵ_{cw}), are expressed as weighted mean values using the factor:

$$\tau_{Rcw} = (1-p)\tau_{Rc} \tag{7}$$

$$\epsilon_{cw} = (1-p)\epsilon_{c} + p\epsilon_{w} \tag{8}$$

Of course, the water coverage factor is only an equivalent value, since condensation is almost never uniformly spread on the cover. The equivalent wet fraction of the cover is computed as the ratio of the equivalent condensate film thickness (t_{cf}) to the potentially maximum value (t_{cfmax}) for a particular covering material (Pieters et al., 1996):

$$p = \frac{t_{cf}}{t_{cfmax}} \tag{9}$$

The maximum thickness of the condensate film was determined through experiments (Pieters, 1995). During the simulation, the evolution of the equivalent condensate film thickness is estimated according to the water vapor flux, based on the different states of the film. At the beginning of the condensation, the film thickness, in the case of drop-wise condensation, increases until a certain maximum thickness is reached. If condensation goes on, water runs down the cover at the same rate as condensation is formed. As condensation ceases and evaporation starts, the water film gradually gets thinner and thinner. When all the condensation water has been evaporated, the cover becomes dry and no further evaporation can take place (Pieters et al., 1996).

Heat balances are formulated for all four layers in the GPS. Further, there is a mass transfer equation for the water vapor of the internal air layer. In this way, a system of four heat-balance and one vapor-balance differential equations is formed.

These equations are solved using a very simple and robust numerical method (Wang et al., 1990; Zhu et al., 1998) under a set of boundary conditions: the global and diffuse solar radiation flux densities, the external air temperature and relative humidity, the wind speed, and the subsoil temperature, which is assumed to be constant. These five equations are used to compute the following five unknowns: the cover temperature, the internal air temperature and the internal relative humidity, the soil temperature, and the water temperature for a passive GPS, or the heat input flux density for an active one. From these results, all heat and vapor flux densities in Fig. 1 can be estimated by the simulation model.

The FORTRAN-based computer program of the model works in the frame of the TRNSYS, a computer package developed by Klein et al. (1990) for dealing with time-dependent processes such as heat and mass transfers. Actual computational experiments show that the model is of stable convergence when the time step is less than 0.05 h. Only about 7 min are needed to perform a 7-month simulation on a Pentium 133 PC with a time step of 0.02 h.

3. Model validation

The GGDM has been extensively calibrated and validated against a great number of experimental measurements, under various weather conditions, in the greenhouses located in Gembloux (Belgium), Quebec (Canada) and Dorst (The Netherlands) (de Halleux et al., 1991; Pirard et al., 1993). Experimental data were collected by computer data logger systems. Weather conditions were monitored, including air temperature, relative humidity, wind speed and direction, global and diffuse solar radiation, and thermal radiation. Values were also measured at different places within the greenhouse. These measurements included air temperature and relative humidity, temperatures of the cover, the soil and the vegetation, solar radiation and heating input flux for an active greenhouse (by measuring the flow of the fluid inside the heating pipe and the temperature difference between input and output). Since GGDM is a very complex model, the parameters were calibrated by dividing the model into subsystems. In this way, the calibration processes could be limited to one particular part of the model while the rest was replaced with measured boundary conditions, which made calibration involve a reduced number of parameters (de Halleux et al., 1991).

In validation, the behaviors of the model were analyzed through various sets of data different from those used for calibration. For the passive greenhouses, the mean deviation between the calculated and the measured internal air temperatures is less than 1.0°C with a standard deviation less than 1.5°C (de Halleux, 1989; de Halleux et al., 1991; Pirard et al., 1993). For the active greenhouses, the instantaneous heating load is predicted within 10% (de Halleux et al., 1991). As an example, Fig. 2 gives the comparative values of the calculated and measured temperatures of the internal air of a greenhouse. The calculated temperature matches the measured one satisfactorily except for the night of 16–17 January. This discrepancy is mainly the result of a weak estimation of the sky radiation temperature during that period,

according to de Halleux et al. (1991). A detailed description of the methods and results of GGDM calibration and validation can be found in de Halleux (1989), de Halleux et al. (1991) and Pirard et al. (1993).

The aquaculture pond model of Zhu et al. (1998) was tested using data collected in two ponds in the Beijing suburbs. The coefficient of determination between simulated and measured water temperatures was higher than 0.90. The averaged absolute error of water temperature and its standard deviation were lower than 0.17 and 0.18°C, respectively.

The parameters that need to be re-valued in the GPS model are those of the water and soil layers (Table 2) because the vegetation in the GGDM is replaced with pond water. There are several soil layers to be considered in the GGDM; these have different properties (density, heat capacity, and thermal diffusivity) because soil density and water content evolve with depth. However, in the GPS, these parameters vary much less with soil depth because the soil is densified and water saturated by the pond water. Therefore, only one soil layer is considered in the GPS model. The soil parameters in the GPS take the same values as those of the last soil layer in the GGDM (de Halleux et al., 1991) (Table 2). For the water layer, its density and thermal capacity are commonly known and the thermal emissivity is also readily available (Fritz et al., 1980; Losordo and Piedrahita, 1991). The water parameters in Table 2 were used in the pond model of Zhu et al. (1998).

4. Simulation results and discussions

Simulations are carried out for a GPS with the air leakage rate of 0.15 per hour for three different days and climatic conditions: 17 January (clear), 18 January (overcast) and 15 March (cloudy), which are selected from the so-called 'typical

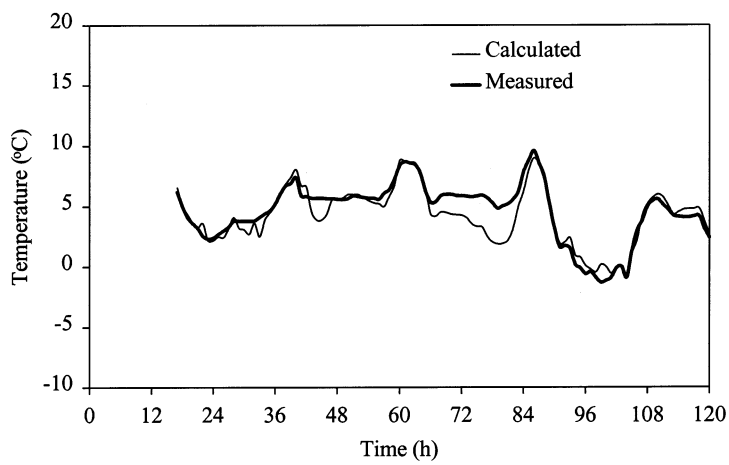

Fig. 2. An example of the validation results of the Gembloux Greenhouse Dynamic Model: predicted versus measured air temperatures inside a greenhouse (after de Halleux et al., 1991).

Table 2
Parameters in the greenhouse pond system model

Parameter	Value	Ref.
Water		
Thermal emissivity (–)	0.97	Fritz et al. (1980), Losordo and Piedrahita (1991)
Mass density (kg m^{-3})	1000	
Mass thermal capacity (J kg^{-1} $°C^{-1}$)	4186	
Soil		
Thermal conductivity (W m^{-1} $°C^{-1}$)	2.0	de Halleux et al. (1991)
Mass density (kg m^{-3})	2000	de Halleux et al. (1991)
Mass thermal capacity (J kg^{-1} $°C^{-1}$)	1500	de Halleux et al. (1991)
Simulation conditions		
Site latitude (°N)	51.8	
Air leakage rate (h^{-1})	0.15	
Soil layer thickness (m)	0.5	
Constant subsoil temperature (°C)	10	
Pond water depth (m)	1.0	
Set point water temperature (°C)	20	

reference year' (Dogniaux et al., 1978). This allows us for a comparison of the thermal characteristics among GPSs with different coverings under various climatic conditions. For instance, there is a significant cloudy period from 11:00 to 14:00 on 15 March, an otherwise serene day. Abrupt changes like this provide an excellent example of the dynamic thermal behaviors of the GPS model.

The inputs of site conditions and simulation parameters are listed in Table 2, where the constant subsoil temperature is considered to equal the annual mean ambient air temperature (de Halleux et al., 1985). In order to perform a comparison among different GPS claddings, four covering materials are adopted for simulation: polyethylene (0.0001 m thick), polyvinyl chloride (0.0001 m), standard glass (0.004 m) and low emissivity glass (0.004 m). The spectral properties of these materials, measured by Nijskens et al. (1985), are given in Table 3. The low emissivity glass, a very expensive material, is introduced here just as a reference for the condensation-wet polyethylene in the far infrared spectral properties.

Fig. 3 shows the simulated temperatures and internal relative humidity of the passive polyethylene GPS for the three selected days. The temperatures rank in the decreasing order: soil, water, internal air, and cover on 17 and 18 January. Due to the large heat-holding capacity of the water and the soil layer, their temperatures are quite stable, and the variation of the internal air temperature is also small. During the night, the GPS can keep the internal air temperature a few degrees higher as compared to a horticultural greenhouse (Deltour et al., 1985). The internal relative humidity is always near 100% due to the continuous evaporation of the water from its surface.

The relative importance of the heat flux terms changes with weather conditions, covering materials, and GPS types (passive or active). Fig. 4 presents the diurnal mean values of the heat flux densities in the passive polyethylene GPS on the three selected days. It is quite clear that, besides solar radiation, the convection between the cover and the external air (V_{ce}), the thermal radiation between the cover and the sky (R_{csky}), and between the water surface and the cover (R_{wc}) are the major heat fluxes. Convection heat fluxes generally flow from the water to the internal air, then to the cover, and finally to the external air (Fig. 4). The flux between the cover and the external air is normally a heat loss. However, it may also be a gain when the cover temperature is lower than the outside air temperature. This could happen on a clear and cold day (such as 17 January in Figs. 4 and 6) when the cover has lost a large amount of thermal radiation heat to the sky.

In the active GPS, the three flux terms above are the key heat losses. For a glass covered GPS, the thermal radiation between the cover and the sky is the most important flux on a clear and cold day (17 January in Fig. 5). It becomes lower than the convection between the cover and the external air on an overcast day (18 January in Fig. 5). The polyethylene GPS, like the one with low emissivity glass, has a lower radiation loss from the cover to the sky, but its convection between the cover and the external air is higher as compared with the glass GPS (Fig. 5). Generally speaking, the heat energy requirement of the active polyethylene GPS is

Table 3
Spectral properties of the tested covering materials (all parameters are dimensionless) (after Nijskens et al., 1985)

Parameters	Beam solar radiation (normal incidence)	Diffuse solar radiation	Thermal radiation
Polyethylene (0.0001 m)			
Transmissivity	0.89	0.80	0.42
Reflectivity	0.10	0.10	0.05
Emissivity			0.53
Polyvinyl chloride (0.0001 m)			
Transmissivity	0.91	0.81	0.33
Reflectivity	0.07	0.09	0.05
Emissivity			0.62
Glass (0.004 m)			
Transmissivity	0.84	0.78	0.00
Reflectivity	0.08	0.04	0.10
Emissivity			0.90
Low emissivity glass (0.004 m)			
Transmissivity	0.77	0.78	0.00
Reflectivity	0.10	0.04	0.10
Emissivity (outside/inside)			0.22/0.90

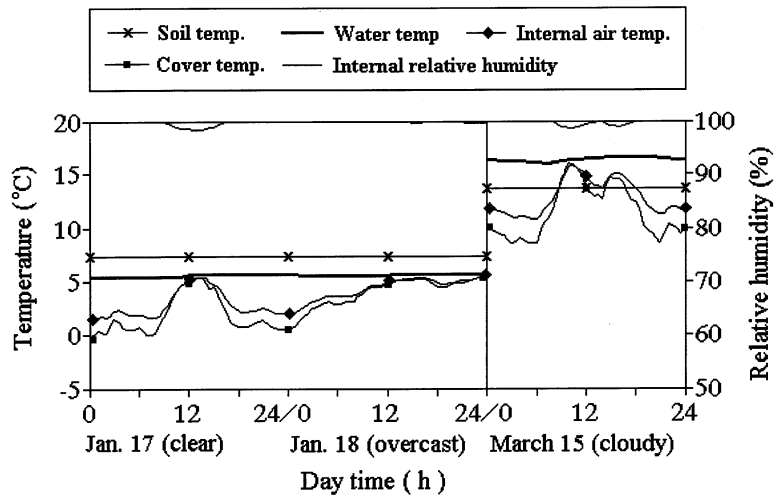

Fig. 3. Simulated temperatures and relative humidity in a passive polyethylene covered pond system.

more than that of the low emissivity glass GPS, but less than that of the glass GPS (Fig. 5).

Latent heat transfer is caused by convection transfer of water vapor. The flux is mostly from the water surface to the internal air and then to the inner surface of the cover or to the external air (Figs. 4 and 7). Because water evaporation creates a high water vapor content in the internal air, the latent heat flux density between the cover and the internal air is always positive unless the cover temperature is higher than the internal air temperature, due to a significant solar radiation level

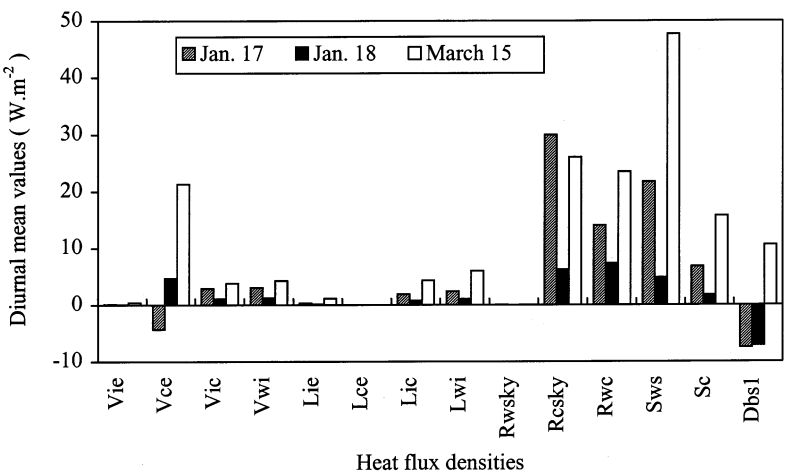

Fig. 4. Diurnal mean values of the heat flux densities in a passive polyethylene covered pond system (see Appendix A for symbols).

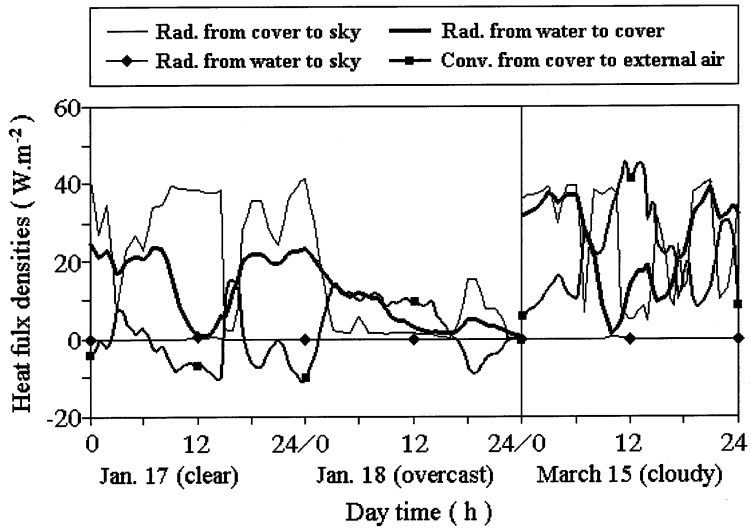

Fig. 5. Evolution of the significant heat flux densities in a passive polyethylene covered pond system.

(17 January and 15 March in Fig. 7). This means that condensation appears very frequently on the inner cover surface. Latent heat flux density between the cover and the external air can be neglected since it rarely appears, according to Figs. 4 and 7. If we consider only air leakage, both latent and convection heat exchanges between internal and external air are quite small, but they are always heat losses for the GPS. The latent heat flux densities themselves are generally very low, but water

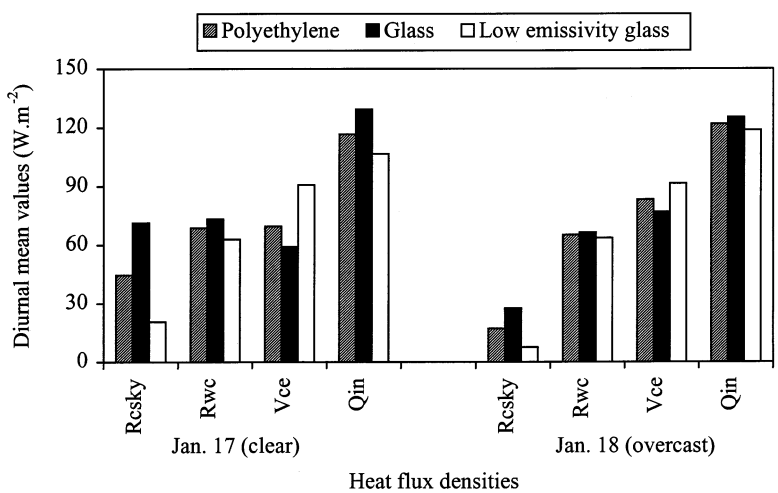

Fig. 6. Major heat flux densities in active greenhouse pond systems with different covering materials when water temperature threshold is set at 20°C (see Appendix A for symbols).

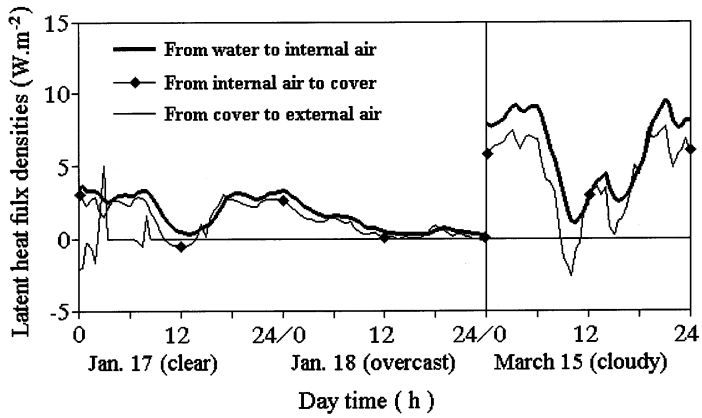

Fig. 7. Evolution of the latent heat flux densities in a passive polyethylene covered pond system.

vapor condensation on the cover surface is very important for the heat budget balance of a greenhouse, especially for a covering material highly transparent to thermal radiation. For example, the thermal radiation transmissivity of polyethylene drops from 0.42 to zero when a dry surface is completely wet by condensation. This is the reason the thermal radiation heat flux between the water surface and the sky (R_{wsky}) is near zero for the polyethylene cover (Figs. 4 and 6).

Thermal radiation heat flux densities depend on the emissivities of the materials and the temperature difference between the two surfaces. The heat flux density between the cover and the sky (R_{csky}), strongly influenced by the cloudiness of the sky, is a major heat loss for the GPS. The radiation flux density between the water and the cover (R_{wc}) is a very significant heat loss for the water, and consequently also a major heat source for the cover (Figs. 4 and 6).

Solar radiation is the main heat source for both cover and water (Fig. 4). The global solar energy is 4.62, 0.69 and 7.93 MJ m^{-2} on 17 and 18 January and 15 March, respectively, of which 40.6, 60.7 and 51.9% reach the water, 12.7, 22.5 and 17.1% are absorbed by the cover, and the others are reflected by the cover.

Subsoil could also supply heat energy for the water of a passive GPS through conduction on very cold days (17 and 18 January in Fig. 4).

Table 4 gives the simulation results of both passive and active GPSs, with different covering materials, from 1 October to 29 April of the 'typical reference year'. For the passive polyethylene GPS, the diurnal mean water temperature is mostly higher than the internal air temperature, which is higher than the external air temperature. The water temperature fluctuates much less than the air temperature. The lowest water temperature (4.4°C) appears on 11 January (Fig. 8), a few days later than the minimum instantaneous external air temperature (-7.7°C) which happens at dawn on 7 and 9 January, respectively. On an average over the 7 months, the passive polyethylene GPS keeps the 1-m pond water 5.2°C warmer than the external air (Table 4).

Table 4
Simulated results for the greenhouse pond systems (GPS) with different coverings over 7 months

Covering material	Polyethylene	PVC	Glass	LEG
Passive GPS				
Mean external air temperature (°C)	6.1	6.1	6.1	6.1
Mean internal air temperature (°C)	8.2	8.2	7.9	9.0
Mean water temperature (°C)	11.3	11.4	10.7	11.6
Active GPS ($T_{wset} = 20$°C)				
Total heat load (MJ m^{-2})	1388.2	1405.4	1528.6	1288.1
Total heat load (%)	90.8	91.9	100	84.3

PVC, polyvinyl chloride; LEG, low emissivity glass; T_{wset}, set point value of water temperature.

For the active polyethylene GPS, the total heat energy demand is 1388.2 MJ m^{-2} over the 7 months when the water temperature threshold is set at 20°C (Table 4). The maximum heat input flux density, occurring on 8 January, is 15.2 MJ m^{-2} day^{-1} (Fig. 9), which is a quite useful datum for the heating system design and management.

From a temperature maintenance (or energy saving) point of view, the polyethylene cover appears better than the glass cover and compares favorably with the low emissivity glass cover (Table 4). This is because the polyethylene cover behaves like the low emissivity glass cover (low emissivity of the outer surface and complete opacity to the thermal radiation) when its transparency to thermal

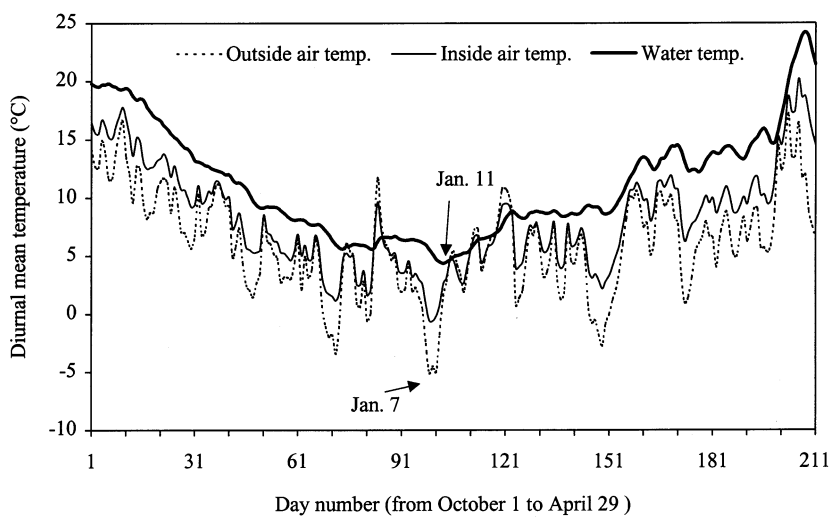

Fig. 8. Diurnal mean values of measured external air temperatures and simulated internal air and water temperatures in a passive polyethylene covered pond system over 7 months.

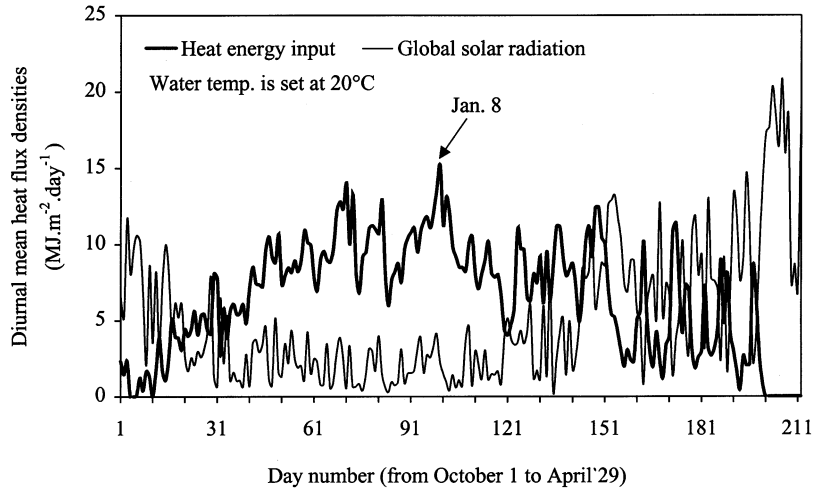

Fig. 9. Diurnal mean values of global solar radiation and heat input flux densities in an active polyethylene covered pond system over 7 months when water temperature threshold is set at 20°C.

radiation is considerably reduced by condensation on the inner cover surface. The polyvinyl chloride cover is almost as effective as the polyethylene one (Table 4).

5. Conclusions

(1) Our dynamic model is developed and seems to be a useful tool for understanding the thermodynamic interactions in the GPS. It can provide an inexpensive means for optimum control of water temperature and evaluation of economic potential for the active GPS.

(2) On average, the passive polyethylene GPS can achieve 5.2°C improvement in the water temperature of a 1-m pond, as compared with the outside air temperature. The night air temperature in the passive GPS remains a few degrees higher than in the horticultural greenhouse.

(3) Besides solar radiation, the convection between the cover and the external air, the thermal radiation between the cover and the sky, and between the water surface and the cover are the three most important heat fluxes in the GPS. Reducing these three heat flux densities is the major method of improving the thermal insulation of the GPS.

(4) Water vapor condensation nearly constantly occurs on the inner cover surface in the GPS, which makes highly thermal-radiation-transparent materials like polyethylene become opaque to thermal radiation. In this case, the PE cover behaves like low emissivity glass.

(5) From a temperature maintenance (or energy saving) point of view, polyethylene and polyvinyl chloride are better materials for the GPS cover than glass.

Acknowledgements

This work was performed at the Faculté Universitaire des Sciences Agronomiques de Gembloux in Belgium under a grant from the European Union and the Fonds Coopération Stagiaires Chinois.

Appendix A. Nomenclature

C_w mass thermal capacity of water (J kg^{-1} °C^{-1})
d characteristic length (m)
D_{bs1} conduction heat flux density from the surface of pond bottom to soil layer 1 (W m^{-2})
D_{s1ss} conduction heat flux density from soil layer 1 to subsoil (W m^{-2})
D_w water depth (m)
Gr Grashof number (dimensionless)
h_v convection heat transfer coefficient (W m^{-2} °C^{-1})
L_{ce} latent flux density between cover and external air (W m^{-2})
L_{ic} latent flux density between internal air and cover (W m^{-2})
L_{ie} latent flux density between internal and external air (W m^{-2})
L_{wi} latent flux density between water surface and internal air (W m^{-2})
Nu Nusselt number (dimensionless)
p equivalent wet fraction of cover surface (dimensionless)
Pr Prandtl number (dimensionless)
Q_{in} heat energy input flux density (W m^{-2})
R_{csky} thermal radiation flux density between cover and sky (W m^{-2})
Re Reynolds number (dimensionless)
RH_e relative humidity of external air (%)
RH_i relative humidity of internal air (%)
R_{wc} thermal radiative flux density between water surface and cover (W m^{-2})
R_{wsky} thermal radiative flux density between water surface and sky (W m^{-2})
S_b solar radiation flux density absorbed by the surface of pond bottom (W m^{-2})
S_c $S_{ec}+S_{wc}$ (W m^{-2})
S_{ce} solar radiation flux density reflected by external cover surface (W m^{-2})
S_{ec} solar radiation flux density absorbed by cover (W m^{-2})
S_g global solar radiation flux density (W m^{-2})
S_w solar radiation flux density absorbed by water (W m^{-2})
S_{wc} solar radiation flux density reflected from water surface and absorbed by cover (W m^{-2})
S_{ws} solar radiation flux density penetrating water surface (W m^{-2})
t time (s)
t_{cf} equivalent thickness of condensate water film on cover surface (m)
t_{cfmax} maximum thickness of condensate water film on cover surface (m)
T_c cover temperature (°C)

T_e external air temperature (°C)
T_i internal air temperature (°C)
T_{s1} temperature of soil layer 1 (°C)
T_{ss} subsoil temperature (°C)
T_{sky} radiative sky temperature (K)
T_w water temperature (°C)
T_{wset} preset water temperature for an active GPS (°C)
V_{bw} convective flux density between pond bottom and water (W m^{-2})
V_{ce} convective flux density between cover and external air (W m^{-2})
V_{ic} convective flux density between internal air and cover (W m^{-2})
V_{ie} convective flux density between internal and external air (W m^{-2})
V_{wi} convective flux density between water surface and internal air (W m^{-2})
ϵ_c thermal emissivity of dry cover surface (–)
ϵ_{cw} equivalent emissivity of cover surface with condensate water (–)
ϵ_w thermal emissivity of water surface (–)
λ thermal conductivity of bulk fluid (W m^{-1} °C^{-1})
ρ_w water density (kg m^{-3})
τ_{Rc} thermal transmissivity of dry cover (–)
τ_{Rcw} equivalent thermal transmissivity of cover with condensate water (–)

References

Bot G.P.A., 1983. Greenhouse climate: from physical processes to a dynamic model. Ph.D. Dissertation, Wageningen Agricultural University, The Netherlands.

Cathcart, T.P., Wheaton, F.W., 1987. Modeling temperature distribution in freshwater ponds. Aquacult. Eng. 6, 237–257.

Cuenco, M.L., 1989. Aquaculture Systems Modeling: An Introduction with Emphasis on Warmwater Aquaculture. International Center for Living Aquatic Resources Management, Manila, Philippines.

de Halleux, D., 1989. Modèle dynamique des échanges énergétiques des serres: étude thèorique et expérimentale (Dynamic model of greenhouse energy exchange: a theoretical and experimental study). Dissertation Doctoral, Faculté Universitaire des Sciences Agronomiques de Gembloux, Belgium.

de Halleux, D., Deltour, J., Nijskens, J., Nisen, A., Coutisse, S., 1985. Dynamic simulation of heat fluxes and temperatures in horticultural and low emissivity glass-covered greenhouses. Acta Hortic. 170, 91–96.

de Halleux, D., Nijskens, J., Deltour, J., 1991. Adjustment and validation of a greenhouse climate dynamic model. Bull. Rech. Agron. Gembloux 26, 429–453.

Deltour, J., de Halleux, D., Nijskens, J., Coutisse, S., Nisen, A., 1985. Dynamic modelling of heat and mass transfer in greenhouses. Acta Hortic. 174, 119–126.

Dogniaux, R., Lemoine, M., Sneyers, R., 1978. Année-type moyenne pour le traitement de problèmes de captation d'énergie solaire (Typical reference year for the treatment of solar energy captation problems). Inst. R. Meteorol. Belg. Bruxelles Misc. Ser. B45, 1–48.

Fritz, J.J., Meredith, D.D., Middleton, A.C., 1980. Non-steady state bulk temperature determination for stabilization ponds. Water Res. 14, 413–420.

Kindelan, M., 1980. Dynamic modeling of greenhouse environment. Trans. ASAE 23, 1232–1239.

Klein, S.A., Beckman, W.A., Cooper, P.I., Duffie, N.A., Freeman, T.L., Mitchell, J.C., Beekman, D.M., Oonk, R.L., Hughes, P.J., Eberlein, M.E., Karman, V.D., Pawelski, M.J., Utzinger, D.M., Duffie, J.A., Brandemuehl, M.J., Arny, M.D., Theilacker, J.C., Morrison, G.L., Clark, D.A., Braun, J.E.,

Evans, B.L., Kummer, J.P., 1990. TRNSYS—a transient system simulation program (version 13.1). Engineering Experiment Station Report 38-13, Solar Energy Laboratory, University of Wisconsin-Madison.

Klemetson, S.L., Rogers, G.L., 1985. Aquaculture pond temperature modeling. Aquacult. Eng. 4, 191–208.

Little, M.A., Wheaton, F.W., 1987. Water temperature prediction in a greenhouse covered aquaculture pond: a progress report. ASAE Paper No. 87-4022.

Losordo, T.M., Piedrahita, R.H., 1991. Modelling temperature variation and thermal stratification in shallow aquaculture ponds. Ecol. Modell. 54, 189–226.

Monteith, J.L., Unsworth, M.H., 1990. Principles of Environmental Physics, 2nd ed. Edward Arnold, London.

Mowla, D., Karimi, G., 1995. Mathematical modelling of solar stills in Iran. Sol. Energy 55, 389–393.

Nijskens, J., Deltour, J., Coutisse, S., Nisen, A., 1984. Heat transfer through covering materials of greenhouses. Agric. For. Meteorol. 33, 193–214.

Nijskens, J., Deltour, J., Coutisse, S., Nisen, A., 1985. Radiation transfer through covering materials, solar and thermal screens of greenhouses. Agric. For. Meteorol. 35, 229–242.

Nijskens, J., de Halleux, D., Deltour, J., 1991. Sensitivity study of a greenhouse climate dynamic model. Bull. Rech. Agron. Gembloux 26, 389–410.

Pieters, J.G., 1995. Influence of condensation on the heat balance and the light transmission of a greenhouse. Ph.D. Dissertation, Gent University, Belgium.

Pieters, J.G., Deltour, J.M., 1997. Performances of greenhouses with the presence of condensation on cladding materials. J. Agric. Eng. Res. 68, 125–137.

Pieters, J.G., Deltour, J.M., Debruyckere, M.J., 1996. Condensation and dynamic heat transfer in greenhouses. Part I: Theoretical model. Agric. Eng. J. 5, 119–133.

Pirard, G., Vancayemberg, F., Deltour, J., 1993. Rapport d'activités de décembre 1993 (Report of activities in December of 1993). Centre d'Etude de la Régulation Climatique des Serres, Gembloux.

Sartori, E., 1996. Solar still versus solar evaporator: a comparative study between their thermal behaviours. Sol. Energy 56, 199–206.

Shawaqfeh, A.T., Farid, M.M., 1995. New development in the theory of the heat and mass transfer in solar stills. Sol. Energy 55, 527–535.

Takakura, T., Jordan, K.A., Boyd, L.L., 1971. Dynamic simulation of plant growth and environment in the greenhouse. Trans. ASAE 14, 964–971.

Wang, S., Deltour, J., Nijskens, J., de Wergifosse, P., 1990. Exact analytical solution of a linear dynamic model of greenhouse climate: the direct cover case. Bull. Rech. Agron. Gembloux 25, 491–520.

Zhu, S., Wang, S., Deltour, J., 1998. A stratification model of aquaculture pond system. Aquacult. Rev. Lett. (in press).